Original Article
Food Science and Technology

ISSN 0101-2061 (Print)
ISSN 1678-457X (Online)

DOI: https://doi.org/10.1590/fst.24822

The influence of microbial bacterial proteins on metabolites in the chilled tan sheep meat

Qianqian HU[1], Junyi ZHAO[1], Ruiming LUO[1*], Liqin YOU[2], Xiaoce ZHAO[1], Chunxia SU[1], Heyu ZHANG[1]

Abstract

This study aims to investigate experimentally the influence of microbial bacterial proteins on microbial metabolites in the chilled storage of Tan Sheep meat based on the surface enhanced laser desorption/ionization-time of flight-mass spectrometry (SELDI-TOF-MS) and gas chromatography-time of flight-mass spectrometry (GC-TOF MS). The correlation analysis of differentially abundant proteins and differential metabolites detected simultaneously in different storage periods has been carried out by heatmap analysis. The results show that 30 differential expressed metabolites were statistically significant. These metabolites were identified as potential spoilage biomarkers. Among of them, 25 differential expressed metabolites can be matched to KEGG metabolic pathways. cyano-amino-acid pathway, pentose phosphate pathway, histidine pathway, purine metabolic pathways, lanine, aspartic acid and glutamate pathway were highly active. Therefore, the differentially abundant proteins contents of microbiology in metabolism can lead to differential effects on metabolic pathways.

Keywords: tan sheep meat; chilled storage; differentially abundant proteins; differential expressed metabolites; metabolic pathway.

Practical Application: This work provides a helpful guidance for the development of microbial prediction and the control technology of meat quality in the production of chilled Tan sheep meat.

1 Introduction

Tan sheep (ovis aries) is a kind of regional breed livestock distributed in Ningxia, China (Gao et al., 2014), whose meat is easily polluted by microorganisms in the process of slaughter and segmentation. Therefore, it is very important to study the growth and metabolism of microorganisms in chilled Tan sheep meat. In recent years, with the development of omics technology, many scholars have studied the microbial diversity and growth metabolism of meat by using proteomics and metabolomics (D'Alessandro et al., 2011).

Generally, food spoilage always occurs at the level of protein macromolecules, and the regulation of protein function plays an important role in the growth of spoilage microorganisms. In 2015, Zhao et al. (2015) identified 335 proteins with at least two unique peptides through the further proteomic analysis of Pu'er tea by using liquid chromatography-mass spectrometry or mass spectrometry (LC-MS/MS) (Zhao et al., 2015). It is found that half of the identified proteins are from Aspergillus, indicating that Aspergillus are the dominant bacterium and a major contributor to solid state fermentation. Martínez-Gomariz et al. (2009) analyzed the proteome changes of Bacillus cereus after the treatment of high hydrostatic pressure (HHP) (Martínez-Gomariz et al., 2009), enzymatic proteins involved in nucleoside metabolism are identified and other proteins involved in carbohydrate metabolism, transport, refolding, amino acid biosynthesis and bacterial flagellum motility can be also affected by the treatment of HHP. Vidal et al. (2020b) investigated the influence of ysine, yeast extract and partial reduction of Sodium Chloride on salted meat, and found the sensory acceptance can be improved by the addition of lysine and yeast extract (Vidal et al., 2020a). In addition, Q methodology can be used to obtain the conceptual representation and sensory profiling of low sodium salted meat (Vidal et al., 2020a), and the dynamic sensorial methods (i.e., Temporal Dominance of Sensations and Temporal Check-all-that-apply) can be used to evaluate the dependence of Bologna sausage with addition of emulsion gel on salt and fat reduction in the dynamic sensorial perception (Paglarini et al., 2020). Nilsson et al. (2012) studied the mechanism of Listeria responding to alkaline treatment by using shotgun proteomics technology (Nilsson et al., 2012), Listeria can effectively regulate intracellular pH and induce the reduction of cell division. Angelakis et al. (2011) identified bacteria in yogurt and other probioticfoods by MALDI-TOF mass spectrometry (Angelakis et al., 2011), and found a large number of live bacteria in the range of 106-109/g in 13 probiotic foods tested (i.e., Lactobacillus casei, Bifidobacterium animalis and Streptococcus thermophilus).

In fact, metabolomics has been developed rapidly and widely used in the fields of microbial identification, metabolic engineering and environmental microorganism. Lu et al. (2012) found that the overexpression of proteins related to the pentose phosphate pathway increases the production of ornithine (Lu et al., 2012). In 2015, Wendler et al. (2016) used the proteomics and

[1]*School of Agriculture, Ningxia University, Yinchuan, Ningxia, P. R. China*
[2]*School of Biological Science and Engineering, North Minzu University, Yinchuan, Ningxia, P. R. China*
**Corresponding author: ruimingluo.nx@163.com*

Received 20 Feb., 2022
Accepted 24 Apr., 2022

metabolomics technology to research the effect of proteins on sugar transport pathway under different conditions, and revealed the cause of differential metabolites (Wendler et al., 2016). Seo et al. (2016) used GC-MS and principal component analysis (PCA) to study the metabolic change of Lactobacillus plantarum in pickle fermentation (Seo et al., 2016), and found that the increase of Lactobacillus plantarum in the fermentation process can lead to the decrease of valine, leucine, citric acid and sucrose. Dai et al. (2016) analyzed the change of metabolites during the fermentation of a black tea by means of nontargeted metabolomics of UPLC-MS, and reported that 61 metabolites can be identified (Dai et al., 2016). Zampieri et al. (2017) studied the effect of the growth environment for bacteria on metabolism, and found that the environment can adjust the metabolic pathway of bacteria, causing the change of metabolites and their intermediates (Zampieri et al., 2017). According to metabolomics analysis of CE-TOF-MS, Muroya et al. (2014) investigated the key compounds and metabolic pathways related to meat quality after pig is slaughtered, and revealed that proteins have an important influence on the metabolic pathways, leading to the change of the types and relative contents of metabolites (Muroya et al., 2014). However, there are few reports in the existing literature on the biochemical mechanism of microbial growth and metabolism during the chilled storage of meat.

In this paper, we focus on the relationship between the differentially abundant bacterial proteins and differentially expressed metabolites, and then discuss the influence of differentially abundant bacterial proteins and differentially expressed metabolites on the metabolic pathway of microorganisms during chilled storage of Tan sheep meat according to proteomics and metabolomics. These results can provide helpful guidance for the development of microbial prediction and meat quality control technology in the production of chilled Tan sheep meat.

2 Material and methods

2.1 Animals and scrapings samples

In the experiment, all methods were carried out in accordance with relevant guidelines formulated by the Ministry of Agriculture of the People's Republic of China, and all experimental protocols were approved by the Ningxia Laboratory Animal Specialized Committee. Freshly slaughtered Tan sheep hind legs (2.5-3.0 kg, totally 24 hind legs) obtained from a local abattoir (Yinchuan, China), were placed into sterile food grade bags and maintained at 0-4 °C, then cooled to -20 °C for 60 min and kept at 0 °C in refrigerator in the laboratory, further sampled at 0, 4, 8 and 12 days, respectively. After 0, 4, 8 and 12 days of storage, samples consisted of the surfaces of whole hind legs for chilled Tan sheep is over an area of 30 * 30 cm^2. Before collecting samples, the frozen collection tubes, tweezers, and knife were disinfected with 70% alcohol, dried, and sealed into a bag. The samples included muscle, connective tissue, blood, fat, etc, need to be operated with sterile experimental equipment in a sterile environment.

For the 0-d sampling, samples (≥ 50 μg each) were collected by rapid scraping 6 hind legs of a freshly slaughtered Tan sheep, three biological duplications were set at each time point, and placed into three frozen tubes (i.e., C0-1-1, C0-1-2, C0-1-3, C0-2-1, C-0-2-2, C-0-2-3, C-0-3-1, C-0-3-2, C-0-3-3, C-0-4-1, C-0-4-2, C-0-4-3, C-0-5-1; C-0-5-2, C-0-5-3, C-0-6-1, C-0-6-2 and C-0-6-3), then immediately frozen in liquid nitrogen and put into a freezer at -80 °C after 1 h. The remainder of the leg was in a box held at 4 °C by ice packs and transported to the laboratory. Then, leg meat was stored in pallet package covered with preservative film and put back into the refrigerator (4 °C) according to the relevant guidelines set by the Ministry of Agriculture of the People's Republic of China. For the 4-d sampling, the samples (≥ 50 μg each) were put into three frozen tubes (i.e., C4-1-1, C4-1-2, C4-1-3, C4-2-1, C4-2-2, C4-2-3, C4-3-1, C4-3-2, C4-3-3, C4-4-1, C4-4-2, C4-4-3, C4-5-1, C4-5-2, C4-5-3, C4-6-1, C4-6-2, C4-6-3) and immediately frozen. For the 8-d and 12-d sampling, the same procedure was followed as at 4-d, the frozen tubes were marked as C8-1-1, C8-1-2, C8-1-3, C8-2-1, C8-2-2, C8-2-3, C8-3-1, C8-3-2, C8-3-3, C8-4-1, C8-4-2, C8-4-3, C8-5-1, C8-5-2, C8-5-3, C8-6-1, C8-6-2, C8-6-3 and C12-1-1, C12-1-2, C12-1-3, C12-2-1, C12-2-2, C12-2-3, C12-3-1, C12-3-2, C12-3-3, C12-4-1, C12-4-2, C12-4-3, C12-5-1, C12-5-2, C12-5-3, C12-6-1, C12-6-2, C12-6-3. A total of 24 tan sheep hind legs were sampled for 8 times, and 3 biological replicates were set at each time point in 4 different periods of 0-d, 4-d, 8-d, 12-d, in order to ensure sufficient high-quality RNA isolation.

2.2 SELDI-TOF-MS: samples preparation

Using the low temperature frozen cell enzyme activity, the collected samples were quenched by liquid nitrogen quenching method, and the freezing time was allowed to rest for 1 min, 2 min, 3 min, 4 min and 5 min, respectively. The thallus was separated by low temperature centrifugation and rapid filtration. Cryogenic centrifugation: The cell quench was frozen and centrifuged at -9 °C for 3 min at 12000 rpm, the supernatant was discarded and the cells were washed with deionized water pre-cooled at 0 °C for 3 times. Rapid filtration method: The cell quencher was quickly filtered by a vacuum pump and the thallus were washed with deionized water pre-cooled at 0 °C, all the above steps were completed within 1 min. The thallus obtained by the two methods were frozen in a refrigerator at -80 °C. The bacteria solution was taken out from the -80 °C refrigerator and placed on an ice box to melt. Prepare two sets of EP (500 μL and 200 μL, the number matches the number of samples to be taken at a time) tubes. Take 20 μL of U9 cracking liquid into 500 μL EP tubes. Take 10 μL of bacterial solution into 500 μL EP tubes containing 20 μL of U9 cracking solution, and mix well. Setting at room temperature for 30 min. Add 370 μL of WCX-2 buffer (NaAC, pH 4.0) to the denatured bacterial sample and mix as soon as possible. Blow off serum samples to avoid air bubbles. Then, the sample should be placed in standby state and waited for machine test.

2.3 SELDI-TOF-MS: statistical analysis

The changes of the differentially abundant proteins in microbial cell and metabolites in Tan sheep during chilled storage were analyzed by SPSS 19.0 statistical software (SPSS Inc., Chicago, IL, U.S.A.) . Then, using the "Pearson" algorithm of R software and SIMCA software (V14.1, MKS Data Analytics Solutions, Umea, Sweden) to perform heatmap analysis of differentially

abundant proteins in bacterial cells and metabolites to find out the correlation between differentially abundant proteins in bacterial cells and metabolites. Therefore, the metabolic pathways of differential expressed metabolites can be found by KEGG database, and the effect of microbial differentially abundant proteins on differential metabolites is also discussed.

2.4 SELDI-TOF-MS: data analysis

The SELDI-TOF-MS platform was used to analyze the differentially abundant proteins of microbial cells on the surface of Tan sheep meat at 0, 4, 8 and 12 days during chilled storage. SPSS (v 19.0) software was used for data pre-processing, set the first step S/N > 5, then the second step S/N > 2, get the peak cluster data, and calculate the differences of each peak in different components (the $P < 0.05$ is the threshold value to screen the differential peaks, and the differential peaks are screened from different sample groups). All differential expression peaks were clustered to determine the interaction between the differential peaks and different samples. In general, the closer the samples on the clustering graph are, the closer the relationship between the differential peaks is. Pick2gene software (Shanghai Minxin Information Technology Co., Ltd.) was used to identify the proteins corresponding to the differential peaks. The SWISS-PROT Database and the EMBL (TrEMBL) database were used to check the differentially abundant proteins of bacterial cell.

2.5 GC-MS: samples preparation

According to You et al. (2018) proposed the storage method of samples (You et al., 2018), GC-MS internal standard solution was prepared with methanol-chloroform solution with a volume ratio of 3 : 1 (Meryer Technologies Co., Ltd., Shanghai, China) and L-2-chlorophenylalanine solution with a concentration of 1 mg/mL. Put the accurately weighed samples collected in 0, 4, 8 and 12 days (50 mg) into 2 mL EP tubes and mixed the internal standard solution with 0.4 mL methanol-chloroform and 20 μL L-2-chlorophenylalanine. The ball mill was used to homogenize the prepared suspension at 65 Hz for 3 min, then put them in centrifuge at the rate of 14,000 g and the temperature of 4 °C for 15 min. Vacuum dried at 37 °C for 3.5 h and blend in 80 μL prepared methoxylamine hydrochloride (Meryer Technologies Co., Ltd., Shanghai, China) at a concentration of 20 mg/mL. After sealed and mixed, the samples were immersed in a constant temperature bath at 80 °C for 20 min. After opening the flask, add 100 μL BSTFA (Regis Technologies, Inc., Morton Grove, USA), then sealed again and immersed in 70 °C constant temperature for 60 min. Added 5μL FAME (Hengbai Biotech Co., Ltd.) into the samples, mixed and cooled to the room temperature.

2.6 GC-MS: metabolites analysis

GC-MS analysis was performed in combination with Agilent 7890 gas chromatography system and Pegasus HT time-of-flight mass spectrometer (LECO, St. Joseph, MI, USA). The carrier gas is helium and the scan rate is 3 mL/min. The initial temperature was maintained at 50 °C for 1 min, then increased to 330 °C at a rate of 10 °C/min, and kept at 330 °C for 5 min. The implantation, transfer line, and ion source temperatures were 280 °C, 280 °C, and 220 °C, respectively. In electron collision mode, the energy was 70 eV, and the solvent delay is 366 s, the mass spectrum data was collected at the rate of 20 spectra/s in the full scan mode of 30 ~ 600 m/z.

2.7 GC-MS: data analysis

The overload peak was removed and the relative content percentage was calculated by area normalization method. Principal component analysis (PCA) and supervised orthogonal partial least squares discriminate analysis (PLS-DA) were analyzed by using SIMCA-P version 13.0 (Umetrics, Sweden) (Zhao et al., 2015). Variables with importance in projection (VIP) values were combined with t-tests to determine the metabolites. "VIP > 1.00", "$p < 0.05$", and "Similarity > 700" were the screening criterion as a potential biomarkers (Lv et al., 2015). 30 differential expressed metabolites and their relative contents were obtained by GC-MS analysis. Metabolites were first converted by logarithm as an input to a hierarchical clustering algorithm, where the distance style is Euclidean and linkage is average (Sun et al., 2017).

3 Results

3.1 Differentially abundant proteins and bacterial cells in chilled tan sheep during storage

SELDI-TOF-MS was used to measure the 16 differentially abundant bacterial proteins associated with microorganisms in chilled Tan sheep meat during storage, the change of the peak area percentage is shown in Table 1.

It can be seen from Table 1 that during the chilled storage, differentially abundant bacterial proteins including Phytophthora protein, NADH-ubiquinone oxidoreductase chain 4L, somatostatin-28, GRF/GHRH growth hormone releasing hormone, Cathelicidins, ATP Synthase F(0) complex subunits C1, ATP synthesis protein, apolipoprotein C-II, prion proteins, apolipoprotein E all show significant changes with the increase of chilled storage time.

3.2 Screening of differential expressed metabolites of microorganisms in chilled tan sheep during storage

In this experiment, the OPLS-DA model variation weight coefficient VIP (Variable Importance in the Projection) value (threshold value > 1) and the student's t-test *p*-value (threshold value < 0.05) were adopted. Select the threshold VIP > 1 and *p*-value < 0.05 to find differential metabolites, and then compare the spectra of these differential metabolites with the LECO/Fiehn metabolic database to identify the potential differential metabolites. The screening results of different groups are shown in Tables 2-4.

Note that peak is the name of each substance obtained qualitatively; Similarity is the degree of matching between the qualitatively obtained substances and these in the standard library; Mass is the nuclear-to-mass ratio of the characteristic ion for the substance; Meanxx is the average of the peak area for each group after normalization; VIP value is the weight of difference by metabolites between the two groups; *p*-value is the result of the student's t test. *p*-value is equal to the probability

Table 1. The change of differentially abundant proteins in tan sheep meat during chilled storage.

Mass-to-charge ratio	protein	ID	0 d	4 d	8 d	12 d
M7823_80	Growth-regulated alpha protein	A0A1V4JWG2	5.50% ± 0.21%	4.97% ± 0.18%	4.29% ± 0.18%	3.98% ± 0.17%
M8414_05	Necrosis-inducing phytophthora protein	A0A0W8CRK9	6.11% ± 0.27%	7.78% ± 0.24%	9.17% ± 0.3%	12.35% ± 0.13%
M10880_9	NADH-ubiquinone oxidoreductase 4L	P33602	6.01% ± 0.17%	8.91% ± 0.27%	9.75% ± 0.32%	10.43% ± 0.32%
M3130_58	Somatostatin-28	O46688	5.06% ± 0.19%	8.67% ± 0.23%	10.23% ± 0.46%	13.48% ± 0.21%
M5109_45	growth hormonereleasing factor	P07217	10.04% ± 0.32%	6.57% ± 0.19%	4.14% ± 0.16%	3.97% ± 0.12%
M6199_14	60S ribosomal protein L40	P14794	5.63% ± 0.22%	5.02% ± 0.14%	4.41% ± 0.17%	3.83% ± 0.15%
M7451_79	Antibacterial peptide	P85078	5.20% ± 0.16%	5.98% ± 0.19%	7.52% ± 0.21%	8.48% ± 0.22%
M7668_64	ATP synthase F(0) complex subunit C1	P68699	5.07% ± 0.17%	6.00% ± 0.11%	7.06% ± 0.39%	8.67% ± 0.17%
M7709_26	ATP synthase subunit	P0AB98	8.49% ± 0.24%	6.36% ± 0.17%	4.29% ± 0.13%	2.34% ± 0.16%
M8136_55	Apolipoprotein C-II	A0A3B4WGI6	5.25% ± 0.15%	6.75% ± 0.15%	7.93% ± 0.06%	8.78% ± 0.15%
M9074_86	prion protein	P31658	5.22% ± 0.13%	6.73% ± 0.14%	8.52% ± 0.12%	11.02% ± 0.17%
M11722_8	thioredoxin	P0AA25	6.01% ± 0.18%	5.14% ± 0.22%	4.75% ± 0.14%	3.99% ± 0.23%
M11870_3	β2microglobulin	Q6QAT4	5.50% ± 0.14%	4.92% ± 0.16%	4.19% ± 0.11%	3.86% ± 0.21%
M12826_1	40S ibosomal protein S26	Q54TL8	5.76% ± 0.16%	5.24% ± 0.21%	4.62% ± 0.08%	4.05% ± 0.19%
M34203_3	Apolipoprotein E	P23930	8.99% ± 0.21%	6.16% ± 0.24%	4.58% ± 0.15%	2.04% ± 0.17%
M38968_8	Annexin V	W5PSZ5	6.17% ± 0.16%	4.80% ± 0.16%	4.54% ± 0.04%	3.95% ± 0.23%

Table 2. Differential expressed metabolites of chilled tan sheep meat during storage for 4-d and 0-d group.

Peak	Similarity	Mass	MEAN 4-d	MEAN 0-d	VIP	P-VALUE	Q-VALUE	UP/DOWN
fumaric acid	955	245	0.049559603	0.148967592	1.19827	0.014203039	0.074211617	↓
D-Glyceric acid	940	189	0.452655273	0.068355163	2.09813	0.005578797	0.056722909	↑
phenylalanine 1	935	218	0.26421188	0.12826593	1.91066	0.000840454	0.028130129	↑
methionine 1	915	176	0.193085597	0.077284905	1.90914	0.000987958	0.028745611	↑
acetanilide 3	890	174	0.016042794	0.035838633	1.68182	0.011972667	0.070629781	↓
aspartic acid 1	886	232	0.078767479	0.022650788	1.87798	0.043086889	0.125072908	↑
Glucose-1-phosphate	879	217	0.199411461	0.302499655	1.65597	0.029773125	0.105513371	↓
D-(glycerol-phosphate)	869	299	0.350854272	0.217432157	1.58972	0.007540953	0.062742051	↑
Inosine-5'-monophosphate	853	169	0.145805445	0.482281053	1.65861	0.001637914	0.030241687	↓
asparagine 4	824	115	0.031170614	0.019762517	1.75942	0.007804362	0.063387527	↑
1,3-diaminopropane	817	174	9.80624E-09	1.53037E-08	1.65748	0.009422178	0.06676379	↓
lysine	792	156	0.05186895	0.019489268	1.99059	0.000609837	0.026683051	↑
2-Hydroxyvaleric acid	735	131	0.005920605	0.026883139	1.75419	0.04296625	0.124918656	↓
terephthalic acid	723	295	0.00816014	1.53037E-08	1.765	0.019103033	0.083963562	↑
5'-methylthioadenosine 1	710	236	0.004652561	0.007968691	1.8403	0.001655017	0.030266431	↓
Isomaltose 1	701	204	0.005889539	0.001352361	1.13718	3.88642E-05	0.007107354	↑

of being considered correct but rejected is equal to the ratio of number of negatives to total number, which was a test probability of sample data. Q-value is a test probability for the inference obtained, which is equal to the probability of rejection, being correct equals false positives/number of presumed positives, and calculated based on P value. Therefore, the Q-value is a re-statistic of P. The full score is 1000, the closer the similarity score is to 1000, the more accurate the qualitative substance is.

Table 3. Differential expressed metabolites of chilled tan sheep meat during storage of 8-d and 4-d group.

Peak	Similarity	Mass	MEAN 8d	MEAN 4d	VIP	P-VALUE	Q-VALUE	UP/DOWN
D-Glyceric acid	940	189	0.048053731	0.452655273	1.65017	0.001070469	0.032725609	↓
L-Malic acid	931	73	1.420178552	3.606278194	1.81226	0.0003746	0.022123872	↓
myo-inositol	908	305	0.644520791	0.938527873	1.42037	0.049925453	0.205160645	↓
ribitol	891	217	0.021838285	0.016814284	1.86774	0.002222764	0.043313654	↑
oxoproline	888	156	3.926525355	6.182043293	1.67271	0.025586181	0.170987658	↓
gluconic acid 1	882	73	0.104425628	0.758667886	1.94603	0.046718527	0.202243948	↓
Glucose-1-phosphate	879	217	0.10350785	0.199411461	1.44722	0.026246916	0.172471092	↓
mannose 1	868	160	0.070703305	0.528706208	1.11036	0.016089506	0.142292192	↓
inosine 5'-monophosphate	853	169	0.031438759	0.145805445	1.49111	0.020073717	0.156320768	↓
fructose-6-phosphate	847	315	0.219088157	0.628467785	1.10596	0.018654934	0.151726499	↓
asparagine 4	824	115	0.011873179	0.031170614	1.98253	0.000720952	0.026636445	↓
citric acid	823	273	0.038713261	0.00784358	1.43791	0.04983366	0.20508128	↑
trans-4-hydroxy-L-proline 2	781	140	0.20108066	0.253564403	1.60727	0.034944576	0.188208925	↓
ribose	769	217	0.053374799	0.12552007	1.6854	0.01756391	0.14790608	↓
1,5-Anhydroglucitol	717	217	0.069081618	0.001116693	1.84208	0.009992748	0.111687401	↑

Table 4. Differential expressed metabolites of chilled Tan sheep meat during storage of 12-d and 8-d group.

Peak	Similarity	Mass	MEAN 12 d	MEAN 8 d	VIP	P-VALUE	Q-VALUE	UP/DOWN
acetanilide 3	890	174	0.031038982	0.012658029	1.70764	0.004057131	0.271344843	↑
taurine	852	326	0.690828681	7.60338E-09	2.09551	0.011736368	0.447217737	↑
ribose	769	217	0.013903507	0.053374799	1.4105	0.039155019	0.58828436	↓
lactose 1	755	204	0.009624694	0.004515707	1.80219	0.002980396	0.271344843	↑
xylose 1	729	117	0.023398229	0.00447303	1.07181	0.033546708	0.575298569	↑
1,5-Anhydroglucitol	717	217	0.021858169	0.069081618	1.70569	0.030751114	0.567349788	↓

In LECO/fiehn metabolism database, when the similarity value is more than 700, the identified metabolites are considered to be exact match, accurate and reliable. When the similarity value is less than 200, the identified metabolites are named with "analyte". When the similarity value is between 200 and 700, the identified metabolites were extrapolated. In this study, the similarity values of all qualitative substances are all greater than 700, indicating that the obtained substances have high matching degree, accuracy and credibility.

As shown in Tables 2-4, 30 differential expressed metabolites were identified in the four groups of microbial samples for chilled Tan sheep meat, and these differences were mainly concentrated on sugars, sugar alcohols, amino acids and their derivatives, and organic acids. Among them, D-Glyceric acid and asparagine were up-regulated at 4 days and down-regulated at 8 days, Glucose-1-phosphate and Inosine-5'-monophosphate showed a decreasing trend at 4 and 8 days during the storage. For 8 and 12 days, the relative concentration of ribitol decreased gradually, the relative concentration of 1, 5-anhydroglucitol increased and then decreased with the extension of storage time. Compared with 0 days, the relative concentration for acetanilide decreased at 4 days, and increased after 12 days.

3.3 Correlation analysis between differentially abundant proteins and differential expressed metabolites

Among the 30 differential expressed metabolites of chilled Tan sheep meat, D-glyceric acid, asparagine, glucose-1-phosphate, inosine-5'-monophosphate, ribose and acetanilide were the metabolites that showed two differences in three storage periods. Aspartic acid is the precursor of isoleucine, threonine and lysine in the differential expressed metabolites. The similarity value of phenylalanine in the differential metabolite is greater than 900, and the variation weight coefficient VIP value of OPLS-DA model is large, so d-glycerine, asparagine, glucose-1-phosphate, inosine-5'-monophosphate, acetanilide ribose, aspartic acid and phenylalanine were used as the differential metabolites to analyze the correlation between the differential expressed metabolites and differentially abundant bacterial proteins. The "spearman" algorithm of R software was used to calculate the correlation. For brevity, we have divided the mass-to-charge ratio that represents protein as shown in Table 1 into two cases (i.e., case 1 and case 2). Therefore, the results of correlation coefficient matrix for case 1 and case 2 are shown in Tables 5 and 6, respectively. The results of correlation *p*-value matrix for case 1 and case 2 are shown in Tables 7 and 8, respectively.

Table 5. Correlation coefficient matrix of differentially abundant proteins and differential expressed metabolites for case 1.

Variables	Correlation Matrix								
	M7823-80	M8414-05	M10880-9	M3130-58	M5109-45	M6199-14	M7451-79	M7668-64	M7709-26
D-Glyceric acid	-0.4464	-0.2714	-0.2464	-0.2571	0.4821	-0.3642	-0.5678	-0.3607	0.2964
asparagine	-0.5571	-0.3821	-0.2071	-0.3321	0.5857	-0.3714	-0.6214	-0.3892	0.3785
Glucose-1-phosphate	-0.0571	-0.9142	-0.7928	-0.8107	0.5178	-0.425	-0.4428	-0.7464	0.8642
inosine 5'-monophosphate	0.0392	-0.8821	-0.7392	-0.8	0.4892	-0.3714	-0.3928	-0.7357	0.8214
ribose	-0.375	-0.3857	-0.3071	-0.4357	0.4535	-0.3214	-0.375	-0.2428	0.5
acetanilide 3	0.2357	-0.675	-0.7357	-0.875	0.675	-0.4464	-0.2964	-0.3535	0.7785
aspartic acid 1	0.0607	0.5857	0.5214	0.4392	-0.2035	0.125	0.1928	0.4285	-0.3964
phenylalanine 1	0.078571429	0.585714286	0.517857143	0.392857143	-0.178571429	0.146428571	0.2142 85714	0.496428571	-0.453571429

Table 6. Correlation coefficient matrix of differentially abundant proteins and differential expressed metabolites for case 2.

Variables	Correlation Matrix						
	M8136-55	M9074-86	M11722-8	M11870-3	M12826-1	M34203-3	M38968-8
D-Glyceric acid	-0.5392	-0.5428	0.7607	0.6	0.5142	0.3214	-0.5107
asparagine	-0.5678	-0.5035	0.8214	0.8464	0.65	0.475	-0.7071
Glucose-1-phosphate	-0.5	-0.5928	0.4821	0.5571	0.6821	0.625	-0.3571
inosine 5'-monophosphate	-0.3428	-0.55	0.3678	0.4321	0.6214	0.5428	-0.1821
ribose	-0.5714	-0.4964	0.6642	0.6142	0.5	0.5321	-0.7071
acetanilide 3	-0.5571	-0.4571	0.3	0.1928	0.4892	0.2464	-0.3142
aspartic acid 1	0.1785	0.1642	0.1285	-0.2	-0.2678	-0.44641	-0.2642
phenylalanine 1	0.1571	0.2214	0.0785	-0.2357	-0.2464	-0.5035	-0.175

Table 7. Correlation *p*-value matrix of differentially abundant proteins and differential expressed metabolites for case 1.

Variables	*p*-value								
	M7823-80	M8414-05	M10880-9	M3130-58	M5109-45	M6199-14	M7451-79	M7668-64	M7709-26
D-Glyceric acid	0.0972	0.3268	0.3748	0.3537	0.0711	0.1823	0.0298	0.1869	0.2826
asparagine	0.0335	0.1606	0.4577	0.2263	0.0242	0.1734	0.0155	0.1524	0.1648
Glucose-1-phosphate	0.8424	0	0.0006	0.0003	0.0506	0.1159	0.1001	0.0020	0
inosine 5'-monophosphate	0.8929	0	0.0023	0.0005	0.0665	0.1734	0.1484	0.0025	0.00025
ribose	0.1691	0.1565	0.2649	0.1062	0.0915	0.2424	0.1691	0.3819	0.0602
acetanilide 3	0.3965	0.0072	0.0025	0	0.0072	0.0972	0.2826	0.1963	0.0009
aspartic acid 1	0.8324	0.0242	0.0488	0.1031	0.4657	0.6575	0.4900	0.1126	0.1445
phenylalanine 1	0.7826	0.0242	0.0506	0.1484	0.5235	0.6023	0.4420	0.0622	0.0915

Table 8. Correlation *p*-value matrix of differentially abundant proteins and differential expressed metabolites for case 2.

Variables	*p*-value						
	M8136-55	M9074-86	M11722-8	M11870-3	M12826-1	M34203-3	M38968-8
D-Glyceric acid	0.0406	0.0391	0.0015	0.0204	0.0524	0.2424	0.0542
asparagine	0.0298	0.0581	0.0002	6.0047	0.0105	0.0758	0.0043
Glucose-1-phosphate	0.0602	0.0222	0.0711	0.0335	0.0065	0.0148	0.1916
inosine 5'-monophosphate	0.2109	0.0362	0.1778	0.1094	0.0155	0.0391	0.5150
ribose	0.0286	0.0622	0.0085	0.0170	0.0602	0.0437	0.0043
acetanilide 3	0.0335	0.0887	0.2766	0.4900	0.0665	0.3748	0.2535
aspartic acid 1	0.5235	0.5579	0.6482	0.4737	0.3334	0.0972	0.3401
phenylalanine 1	0.5755	0.4265	0.7826	0.3965	0.3748	0.0581	0.5320

Figure 1 shows the differential expressed metabolites-differentially abundant proteins correlation heatmap, the red color (corr = 1) means a positive correlation, the blue color (corr = -1) means a negative correlation and the white color (corr = 0) means no correlation. The relevant data with *p*-value less than 0.05 are represented by "*" in the graph. The darker the color is, the greater the correlation is. The horizontal axis showed differentially abundant proteins and the vertical axis showed differential expressed metabolites. It can be seen from the heatmap that the proteins highly associated with Acetanilide are NADH-ubiquinone oxidoreductase chain 4L (M10880-9), somatostatin-28 (M3130-58), and ATP synthesis protein (M7709 -26). The differential protein somatostatin-28 was negatively correlated with the differential metabolites, while the ATP synthesis protein were positively correlated with differential metabolites. The differential related proteins associated with asparagine to a greater extent were keratin-associated protein 3-1 (M6658-62), thioredoxin (M11722-8), and macrophage migration inhibitory factor (M12261-6). Glucose-1-phosphate, phenylalanine, and 5'-inosinic acid (Inosine-5'-monophosphate) and NADH-ubiquinone oxidoreductase chain 4L, somatostatin -28 were positively correlated with Necrosis-inducing Phytophthora protein (M8414-05), and negatively correlated with keratin-associated protein 8-1 and ATP synthesis protein. The main reason may be that the tricarboxylic acid cycle, phenylalanine metabolism, and glyceride metabolism in the metabolic pathways are different during different storage times. Due to the succession of Pseudomonas and Enterobacter, the related metabolites are also different.

3.4 Analysis of metabolic pathways of differential metabolites

The above differential expressed metabolites were mapped to KEGG database to obtain the metabolic pathways corresponding to differential expressed metabolite. The analysis of metabolic pathways of differential metabolites was shown in Table 9. In different storage periods, there were 30 differentially expressed metabolites with similarity values greater than 700, and 22 differentially expressed metabolites could accurately match metabolic pathways. The metabolic pathways of 5'-inosine-5'-monophosphate, Isomaltose and oxoproline were obtained by referring to related literatures. KEGG database could not find the related metabolic pathways, which may be because the information of these compounds was not included in the bacterial metabolic pathways database.

4 Discussion

4.1 Microbial community succession of tan sheep meat during chilled storage

During the storage, the number of Pseudomonas increased rapidly from 8.86% to 26.23%, and reached 37.16% on the 8th day. This is because Pseudomonas is a kind of aerobic gram-negative bacteria, so the growth rate of Pseudomonas is the fastest under the aerobic condition of tray packaging storage, which is almost not affected by temperature and other microorganisms. Meanwhile, the glucose produced in the process of meat maturing also provides favorable conditions for the growth of Pseudomonas. When the total number of bacteria reaches 108 cfu/cm^2, due to the supply of glucose could not meet the growth demand, Pseudomonas began to use the amino acid of bacterial protein as the growth matrix to generate sulfur compounds, esters, acids and other spoilage products with peculiar smell. At the same time, the growth rate of Enterobacter was slower than that of Pseudomonas, but it still accounts for a certain proportion. Enterobacter is facultative anaerobes, which can ferment glucose and produce acid and gas. Under the condition of cold storage in tray packaging, Enterobacter continue to multiply on glucose and glucose-6-phosphate as growth substrates.

4.2 Correlation between differentially abundant bacterial proteins and differential expressed metabolites of chilled tan sheep meat

The results of 3.4 showed that there was a correlation between microbial differential protein and ifferential metabolite in chilled Tan sheep meat. In this part, we analyzed the reason

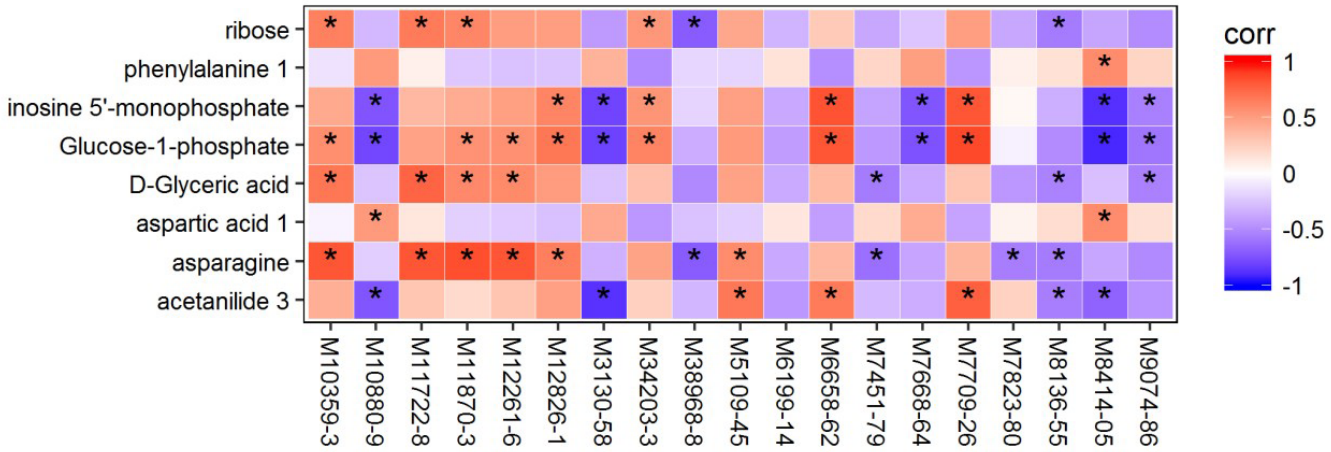

Figure 1. Differential expressed metabolites-differentially abundant proteins correlation heatmap. *Represents the relevant data with p-value less than 0.05.

Table 9. Analysis of metabolic pathway of differential expressed metabolites.

Differential metabolites	Metabolic pathway
fumaric acid	Citrate cycle
	Arginine biosynthesis
	Alanine aspartate and glutamate methabolism
	Tyrosine methabolism
	Phenylalanine methabolism
	Butanoate methabolism
	Nicotinate and Nicotinamide methabolism
D-Glyceric acid	Pentose phosphate pathway
	Glycine serine and threonine methabolism
	Glycerolipid methobolism
	Glyoxylate and dicarboxylate methabolism
	Methane methabolism
phenylalanine 1	Phenylalanine methabolism
methionine 1	Cysteine and methionine methabolism
aspartic acid 1	Alanine aspartate and glutamate methabolism
	Histidine methabolism
	Cyanoamino acid methabolism
asparagine 4	Alanine aspartate and glutamate methabolism
	Cyanoamino acid methabolism
Glucose-1-phosphate	Pentose and glucuronate interconversions
	Embden meyerhof parnas
sn-(glycerol 3-phosphate)	Embden meyerhof parnas
	Glycerolipid methabolism
	Amino sugar and nucleotide sugar methabolism
Inosine-5'-monophosphate	Purine methabolism
lysine	Lysine biosynthesis
1,3-diaminopropane	Glycine serine and threonine methabolism
	β-Alanine methabolism
terephthalic acid	Polycyclic aromatic hydrocarbon degration
5'-methylthioadenosine 1	Cysteine and methionine methabolism
Isomaltose 1	Starch and sucrose methabolism
2-Hydroxyvaleric acid	/
acetanilide 3	/
L-Malic acid	Glyoxylate and dicarboxylate methabolism
	Methane methabolism
	Citrate cycle
myo-inositol	Galactose methabolism
ribitol	Pentose and glucuronate interconversions
oxoproline	Glutathione methabolism
gluconic acid 1	Pentose phosphate pathway
mannose 1	Galactose methabolism
	Amino sugar and nucleotide sugar methabolism
fructose-6-phosphate	Methane methabolism
	Embden meyerhof parnas
	Amino sugar and nucleotide sugar methabolism
citric acid	Citrate cycle
	Glyoxylate and dicarboxylate methabolism
ribose	Pentose phosphate pathway
trans-4-hydroxy-L-proline 2	/
1,5-Anhydroglucitol	/
taurine	/
xylose 1	Galactose methabolism
lactose 1	Pentose and glucuronate interconversions

for the correlation from the following typical differential metabolites and differential proteins. Among them, Phenylalanine metabolism (map00360) produced by Phenylalanine 1 has a growing trend during the storage (Sun et al., 2017), which may be positively related to necrosis-induced Phytophthora protein (M8414-05) content and the increase of storage time. Inosine 5'- monophosphate acid (map00230) metabolized by purine pathway, decreased with the increase of storage time. The results showed that the percentage of bacterial protein with positive correlation decreased, while the percentage of bacterial protein with negative correlation increased. Among them, 40S ribosomal protein S26 (M12826-1), apolipoprotein E (M34203-3), ATP synthesis protein (M7709-26) were beneficial to metabolism. NADH ubiquinone oxidoreductase chain 4L (M10880-9), growth Inhibin-28 (M3130-58), ATPase f (0) complex subunit C1 (M7668-64), and necrotic inducible Phytophthora protein (M8414-05) inhibited the metabolic process. The metabolic pathway of glucose-1-phosphate is the conversion of pentose and glucuronic acid (map00040) (Teufel et al., 2010). The percentage of glucose-1-phosphate peak area decreases with the increase of storage time. The reason is that the percentage of protein content of bacteria with positive correlation tends to decrease, while the percentage of protein content of bacteria with negative correlation tends to increase during storage. Among them, β2-microglobulin (M11870-3), apolipoprotein E (M34203-3), ATP synthesis protein (M7709-26) promote the metabolic process, which is inhibited by NADH ubiquinone oxidoreductase chain 4L (M10880-9), somatostatin-28 (M3130-58), ATP synthetase f (0) complex C1 (M7668-64), necrosis induced Phytophthora protein (M8414-05), and prions (M9074-86). The metabolic pathways of D-glyceric acid include pentose phosphate pathway (map00030) (Cusa et al., 1999), glycine, serine and threonine metabolism (map00260) (Xi et al., 2000) glycolipid metabolism (map00561) (Yew & Gerlt, 2002), glyoxylate metabolism (map00630) (Kouril et al., 2013) and methane metabolism (map00680) (Bursy et al., 2007). With the increase of storage time, the percentage of D-glyceric acid increased, which indicated that thioredoxin (M11722-8) and β2-microglobulin (M11870-3) were beneficial to the production of metabolites. While, antimicrobial peptide (M7451-79), apolipoprotein C-II (M8136-55) and prions (M9074-86) inhibited the production of metabolites. Aspartic acid 1 is metabolized by alanine, aspartic acid and glutamate metabolism (map00250) (Berg et al., 2001), histidine metabolism (map00340) (Khomyakova et al., 2011), cyanoamino acid metabolism (map00460) (Liffourrena et al., 2010). The percentage of aspartic acid 1 content increases with the increase of storage time, indicating that the bacterial protein NADH Ubiquinone which is positively related to the metabolite, is oxidized. The metabolic pathways of asparagine 4 are alanine, aspartic acid, glutamic acid and cyano amino acid. The relative content of asparagine 4 increased from 2.10% on the 0 d to 7.29% on the 4 d and 9.80% on the 8 d, respectively. The related thalli protein thioredoxin (M11722-8), β2-microglobulin (M11870-3), and 40S ribosomal protein S26 (M12826) were positively correlated with asparagine 4-1, while GRF/GHRH growth hormone releasing hormone (M5109-45) decreased slowly. The phospholipid binding protein (M38968-8) and growth regulating α protein (M7823-80) decreased gradually, but the antimicrobial peptide (M7451-79) and apolipoprotein c-II (M8136-55) increased gradually. Thus, these bacterial proteins may affect the metabolism of asparagine 4.

4.3 Analysis of microbial metabolic pathway transformation in chilled tan sheep meat during storage

Through KEGG database retrieval, 11 metabolic pathways such as phenylalanine metabolism, cyano amino acid metabolism, glycine, serine and threonine metabolism, glyceride metabolism, methane metabolism, pentose and glucuronate interconversions, pentose phosphate pathway, alanine, aspartic acid and glutamate metabolism, histidine metabolism, purine metabolism and glyoxylate metabolism can be obtained. These metabolic pathways showed that phenylalanine metabolism, glycine, serine and threonine metabolism pathway have indirect effects on cyanoamino acid metabolism pathway, thioredoxin, β2-microglobulin, and macrophage migration inhibitory factors. Necrosis-inducing Phytophthora protein, 40S ribosomal protein S26, NADH-ubiquinone oxidoreductase chain 4L and GRF/GHRH growth hormone releasing hormone promotes the production of corresponding metabolites in these metabolic pathways, while antibacterial peptides, apolipoprotein C-II, prion proteins, phospholipid-binding proteins, and growth-regulating alpha proteins inhibit these metabolic processes. Because the cyano amino acid metabolic pathway indirectly controlled the alanine, aspartic acid and glutamate metabolic pathways. The glucuronic acid pathway and the pentose phosphate pathway regulate each other, where β2-microglobulin, macrophage migration inhibitory factor, apolipoprotein E, ATP synthesis protein and thioredoxin promote metabolic processes to produce metabolites. NADH ubiquinone oxidoreductase chain 4L, somatostatin-28, ATP synthase f (0) complex subunit C1, necrotizing inducible Phytophthora protein, antimicrobial peptide Apolipoproteins C-II and prions can inhibit the metabolic pathway. Pentose phosphate pathway, histidine metabolism pathway, alanine, aspartic acid and glutamate metabolism pathways affect purine metabolism pathway by affecting different intermediates at different stages of purine metabolism. Thioredoxin, β2-microglobulin, NADH ubiquinone oxidoreductase chain 4L, necrotizing inducible Phytophthora protein, 40S ribosomal protein S26 and GRF/GHRH growth Hormone releasing hormone promotes the production of metabolites, while antimicrobial peptide, apolipoprotein C-II, prion phospholipid binding protein and growth regulating α protein inhibit the production of metabolites. To sum up, Figure 1 shows that bacterial protein can affect microbial metabolic pathway, which may be caused by the influence of that bacterial protein on metabolic pathway of metabolites.

4.4 Effect of microorganism metabolism on quality safety index and edible quality of chilled tan sheep meat

With the extension of storage time, Pseudomonas and Enterobacter proliferate. They use protein, fat, carbohydrate and other nutrients to produce proteases, which leads to the gradual decomposition of protein into a series of products, such as amines, indoles, mercaptans, hydrogen sulfide, and feces. Lipase produced by microorganism can decompose fat into fatty acid, glycerin, aldehyde, ketone and other compounds, resulting in the rancidity of fat. Meanwhile, the carbohydrates are

broken down into various organic acids, or to produce alcohol and CO_2 gas. There are obvious changes in the senses of meat (Bacon et al., 2000), such as color, viscosity, smell, etc. Biogenic amine is a kind of small molecular weight organic compound with nitrogen and biological activity, mainly produced by microorganisms to remove the related free amino acid carboxyl group in food under the catalysis of amino acid decarboxylase. The main biological amines and their precursors related to food spoilage are histidine-histamine, tyrosine-tyramine, lysine-cadaverine, ornithine- putrescine, arginine-arginine, and Spermine (Santos, 1996). In addition, Warthesen et al. (1975) pointed out that diamines such as putrescine and cadaverine can interact with nitrous acid to form nitrosamine compounds, and nitrosamine compounds have been shown to cause cancer (Drabik-Markiewicz et al., 2009). Although low temperature can inhibit the growth of microorganisms, Pseudomonas and Enterobacter are important spoilage microorganisms in low temperature environment because of their special cell structure and cold resistant substances (Moret et al., 2005). With the extension of storage time, Pseudomonas and Enterobacter secrete protease, which continuously decomposes protein in meat and produces alkaline substances such as ammonia and biogenic amine. A large number of studies have shown that dimethylamine is the main diamine product of Pseudomonas, and Enterobacter produces more glutamine, which is also the only product related to Enterobacter in ground beef. When the total number of bacteria in the ground beef is $4 * 10^7$ CFU/g, there is a significant change in the amount of butanediamine and glutamine (Vinci & Antonelli, 2002). These results indicated that the microorganisms would produce and accumulate a lot of compounds, which affected the quality and safety of meat in the later storage period (8-12 days).

5 Conclusion

In this paper, according to proteomic and metabolomic untargeted method, we have identified 16 differentially abundant bacterial proteins and 8 differential expressed metabolites in chilled Tan sheep meat during different storage periods. Differential abundant proteins positively associated with acetanilide are NADH ubiquinone oxidoreductase 4L (M10880-9) and ATP synthesis protein (M7709-26). Differential abundant proteins positively associated with asparagine are keratin associated protein 3-1 (M6658-62), thioredoxin (M11722-8) and macrophage migration inhibitory factor (M12261-6); Differential abundant proteins positively associated with glucose-1-phosphate and inosine-5 '- monophosphate are keratin associated protein 8-1 and ATP synthesis protein, and the negative related proteins are NADH ubiquinone oxidoreductase 4L, somatostatin-28 and necrotizing induced Phytophthora. By matching 25 differential expressed metabolites with metabolic pathways, we found that the cyanoamino acid metabolic pathway, pentose phosphate pathway, histidine metabolic pathway, alanine, aspartic acid and glutamic acid metabolic pathway, and purine metabolism had a higher activity. It can be seen that the change of bacterial protein in Tan sheep meat during chilled storage had an important effect on metabolites, which may be due to the influence of different bacterial proteins contents in metabolism on metabolic pathway.

Conflict of interest

We have no financial and personal relationships with other people or organizations that can inappropriately influence our work, there is no professional or other personal interest of any nature or kind in any product, service and/or company that could be construed as influencing the position presented in, or the review of, the manuscript entitled.

Acknowledgements

This work was supported by the Regional Science Foundation Project of National Natural Science Foundation of China (31460431) and the Regional Key Research and Development Program of Ningxia Hui Autonomous Region of China (2017BY068).

References

Angelakis, E., Million, M., Henry, M., & Raoult, D. (2011). Rapid and accurate bacterial identification in probiotics and yoghurts by MALDI-TOF mass spectrometry. *Journal of Food Science*, 76(8), M568-M572. http://dx.doi.org/10.1111/j.1750-3841.2011.02369.x. PMid:22417598.

Bacon, R. T., Belk, K. E., Sofos, J. N., Clayton, R. P., Reagan, J. O., & Smith, G. C. (2000). Microbial populations on animal hides and beef carcasses at different stages of slaughter in plants employing multiple-sequential interventions for decontamination. *Journal of Food Protection*, 63(8), 1080-1086. http://dx.doi.org/10.4315/0362-028X-63.8.1080. PMid:10945584.

Berg, S., Edman, M., Li, L., Wikström, M., & Wieslander, Å. (2001). Sequence properties of the 1,2-diacylglycerol 3-glucosyltransferase from *Acholeplasma laidlawii* membranes. Recognition of a large group of lipid glycosyltransferases in eubacteria and archaea. *Journal of Biological Chemistry*, 276(25), 22056-22063. http://dx.doi.org/10.1074/jbc.M102576200. PMid:11294844.

Bursy, J., Pierik, A. J., Pica, N., & Bremer, E. (2007). Osmotically induced synthesis of the compatible solute hydroxyectoine is mediated by an evolutionarily conserved ectoine hydroxylase. *Journal of Biological Chemistry*, 282(43), 31147-31155. http://dx.doi.org/10.1074/jbc.M704023200. PMid:17636255.

Cusa, E., Obradors, N., Baldomà, L., Badía, J., & Aguilar, J. (1999). Genetic analysis of a chromosomal region containing genes required for assimilation of allantoin nitrogen and linked glyoxylate metabolism in Escherichia coli. *Journal of Bacteriology*, 181(24), 7479-7484. http://dx.doi.org/10.1128/JB.181.24.7479-7484.1999. PMid:10601204.

D'Alessandro, A., Marrocco, C., Zolla, V., D'Andrea, M., & Zolla, L. (2011). Meat quality of the longissimus lumborum muscle of Casertana and large white pigs: metabolomics and proteomics intertwined. *Journal of Proteomics*, 75(2), 610-627. http://dx.doi.org/10.1016/j.jprot.2011.08.024. PMid:21920477.

Dai, W., Tan, J., Lu, M., Xie, D., Li, P., Lv, H., Zhu, Y., Guo, L., Zhang, Y., Peng, Q., & Lin, Z. (2016). Nontargeted modification-specific metabolomics investigation of glycosylated secondary metabolites in tea (*Camellia sinensis* L.) based on liquid chromatography? High resolution mass spectrometry. *Journal of Agricultural and Food Chemistry*, 64(35), 6783-6790. http://dx.doi.org/10.1021/acs.jafc.6b02411. PMid:27541009.

Drabik-Markiewicz, G., Van den Maagdenberg, K., Mey, E., Deprez, S., Kowalska, T., & Paelinck, H. (2009). Role of proline and hydroxyproline in N-nitrosamine formation during heating in cured

meat. *Meat Science*, 81(3), 479-486. http://dx.doi.org/10.1016/j.meatsci.2008.10.002. PMid:20416602.

Gao, X., Wang, Z., Miao, J., Xie, L., Dai, Y., Li, X., Chen, Y., Luo, H., & Dai, R. (2014). Influence of different production strategies on the stability of color, oxygen consumption and metmyoglobin reducing activity of meat from Ningxia tan sheep. *Meat Science*, 96(2 Pt A), 769-774. http://dx.doi.org/10.1016/j.meatsci.2013.09.026. PMid:24200569.

Khomyakova, M., Bükmez, Ö., Thomas, L. K., Erb, T. J., & Berg, I. A. (2011). Methylaspartate cycle in Haloarchaea. *Science*, 331(6015), 334-337. PMid:21252347.

Kouril, T., Wieloch, P., Reimann, J., Wagner, M., Zaparty, M., Albers, S.-V., Schomburg, D., Ruoff, P., & Siebers, B. (2013). Unraveling the function of the two Entner–Doudoroff branches in the thermoacidophilic Crenarchaeon Sulfolobus solfataricus P2. *The FEBS Journal*, 280(4), 1126-1138. http://dx.doi.org/10.1111/febs.12106. PMid:23279921.

Liffourrena, A. S., Salvano, M. A., & Lucchesi, G. I. (2010). *Pseudomonas putida* A ATCC 12633 oxidizes trimethylamine aerobically via two different pathways. *Archives of Microbiology*, 192(6), 471-476. http://dx.doi.org/10.1007/s00203-010-0577-5. PMid:20437165.

Lu, D., Liu, J., & Mao, Z. (2012). Engineering of Corynebacterium glutamicum to enhance L-ornithine production by gene knockout and comparative proteomic analysis. *Chinese Journal of Chemical Engineering*, 20(4), 731-739. http://dx.doi.org/10.1016/S1004-9541(11)60242-5.

Lv, M., Sun, J., Wang, M., Huang, W., Fan, H., Xu, F., & Zhang, Z. (2015). GC–MS based metabolomics study of stems and roots of Ephedra sinica. *Journal of Pharmaceutical and Biomedical Analysis*, 114, 49-52. http://dx.doi.org/10.1016/j.jpba.2015.04.035. PMid:26004227.

Martínez-Gomariz, M., Hernáez, M. L., Gutiérrez, D., Ximénez-Embún, P., & Préstamo, G. (2009). Proteomic analysis by Two-Dimensional Differential Gel Electrophoresis (2D DIGE) of a high-pressure effect in Bacillus cereus. *Journal of Agricultural and Food Chemistry*, 57(9), 3543-3549. http://dx.doi.org/10.1021/jf803272a. PMid:19338277.

Moret, S., Smela, D., Populin, T., & Conte, L. S. (2005). A survey on free biogenic amine content of fresh and preserved vegetables. *Food Chemistry*, 89(3), 355-361. http://dx.doi.org/10.1016/j.foodchem.2004.02.050.

Muroya, S., Oe, M., Nakajima, I., Ojima, K., & Chikuni, K. (2014). CE-TOF MS-based metabolomic profiling revealed characteristic metabolic pathways in postmortem porcine fast and slow type muscles. *Meat Science*, 98(4), 726-735. http://dx.doi.org/10.1016/j.meatsci.2014.07.018. PMid:25105492.

Nilsson, R. E., Latham, R., Mellefont, L., Ross, T., & Bowman, J. P. (2012). MudPIT analysis of alkaline tolerance by Listeria monocytogenes strains recovered as persistent food factory contaminants. *Food Microbiology*, 30(1), 187-196. http://dx.doi.org/10.1016/j.fm.2011.10.004. PMid:22265300.

Paglarini, C. S., Vidal, V. A. S., Santos, M., Coimbra, L. O., Esmerino, E. A., Cruz, A. G., & Pollonio, M. A. R. (2020). Using dynamic sensory techniques to determine drivers of liking in sodium and fat-reduced Bologna sausage containing functional emulsion gels. *Food Research International*, 132, 109066. http://dx.doi.org/10.1016/j.foodres.2020.109066. PMid:32331676.

Santos, M. H. S. (1996). Biogenic amines: their importance in foods. *International Journal of Food Microbiology*, 29(2-3), 213-231. http://dx.doi.org/10.1016/0168-1605(95)00032-1. PMid:8796424.

Seo, S.-H., Park, S.-E., Yoo, S.-A., Lee, K. I., Na, C.-S., & Son, H.-S. (2016). Metabolite profiling of Makgeolli for the understanding of yeast fermentation characteristics during fermentation and aging. *Process Biochemistry*, 51(10), 1363-1373. http://dx.doi.org/10.1016/j.procbio.2016.08.005.

Sun, H., Wang, B., Wang, J., Liu, H., & Liu, J. (2017). Biomarker and pathway analyses of urine metabolomics in dairy cows when corn stover replaces alfalfa hay. *Journal of Animal Science and Biotechnology*, 7, 49.

Teufel, R., Mascaraque, V., Ismail, W., Voss, M., Perera, J., Eisenreich, W., Haehnel, W., & Fuchs, G. (2010). Bacterial phenylalanine and phenylacetate catabolic pathway revealed. *Proceedings of the National Academy of Sciences*, 107(32), 14390-14395. http://dx.doi.org/10.1073/pnas.1005399107. PMid:20660314.

Vidal, V. A. S., Santana, J. B., Paglarini, C. S., Silva, M. A. A. P., Freitas, M. Q., Esmerino, E. A., Cruz, A. G., & Pollonio, M. A. R. (2020a). Adding lysine and yeast extract improves sensory properties of low sodium salted meat. *Meat Science*, 159, 107911. http://dx.doi.org/10.1016/j.meatsci.2019.107911. PMid:31474317.

Vidal, V. A., Paglarini, C. S., Freitas, M. Q., Coimbra, L. O., Esmerino, E. A., Pollonio, M. A., & Cruz, A. G. (2020b). Q methodology: an interesting strategy for concept profile and sensory description of low sodium salted meat. *Meat Science*, 161, 108000. http://dx.doi.org/10.1016/j.meatsci.2019.108000. PMid:31707157.

Vinci, G., & Antonelli, M. L. (2002). Biogenic amines: quality index of freshness in red and white meat. *Food Control*, 13(8), 519-524. http://dx.doi.org/10.1016/S0956-7135(02)00031-2.

Warthesen, J. J., Scanlan, R. A., Bills, D. D., & Libbey, L. M. (1975). Formation of heterocyclic N-nitrosamines from the reaction of nitrite and selected primary diamines and amino acids. *Journal of Agricultural and Food Chemistry*, 23(5), 898-902. http://dx.doi.org/10.1021/jf60201a004. PMid:1159192.

Wendler, S., Otto, A., Ortseifen, V., Bonn, F., Neshat, A., Schneiker-Bekel, S., Wolf, T., Zemke, T., Wehmeier, U. F., Hecker, M., Kalinowski, J., Becher, D., & Pühler, A. (2016). Comparative proteome analysis of Actinoplanes sp. SE50/110 grown with maltose or glucose shows minor differences for acarbose biosynthesis proteins but major differences for saccharide transporters. *Journal of Proteomics*, 131, 140-148. http://dx.doi.org/10.1016/j.jprot.2015.10.023. PMid:26597626.

Xi, H., Schneider, B. L., & Reitzer, L. (2000). Purine catabolism in Escherichia coli and function of xanthine dehydrogenase in purine salvage. *Journal of Bacteriology*, 182(19), 5332-5341. http://dx.doi.org/10.1128/JB.182.19.5332-5341.2000. PMid:10986234.

Yew, W. S., & Gerlt, J. A. (2002). Utilization of L-ascorbate by Escherichia coli K-12: assignments of functions to products of the yjf-sga and yia-sgb operons. *Journal of Bacteriology*, 184(1), 302-306. http://dx.doi.org/10.1128/JB.184.1.302-306.2002. PMid:11741871.

You, L., Guo, Y., Luo, R., Fan, Y., Zhang, T., Hu, Q., & Bo, S. (2018). Spoilage marker metabolites and pathway analysis in chilled tan sheep meat based on GC-MS. *Food Science and Technology Research*, 24(4), 635-651. http://dx.doi.org/10.3136/fstr.24.635.

Zampieri, M., Zimmermann, M., Claassen, M., & Sauer, U. (2017). Nontargeted metabolomics reveals the multilevel response to antibiotic perturbations. *Cell Reports*, 19(6), 1214-1228. http://dx.doi.org/10.1016/j.celrep.2017.04.002. PMid:28494870.

Zhao, M., Zhang, D.-l., Su, X.-q., Duan, S.-m., Wan, J.-q., Yuan, W.-x., Liu, B.-y., Ma, Y., & Pan, Y.-h. (2015). An integrated metagenomics/metaproteomics investigation of the microbial communities and enzymes in solid-state fermentation of Pu-erh tea. *Scientific Reports*, 5(1), 10117. http://dx.doi.org/10.1038/srep10117. PMid:25974221.